Hindawi
Advances in Materials Science and Engineering
Volume 2022, Article ID 1506483, 7 pages
https://doi.org/10.1155/2022/1506483

Research Article

Axial Compression Behavior of Rubberized Concrete-Filled Square Steel Tubular Columns after Exposed to High Temperatures

Lanlan Yan,[1] Jiongfeng Liang,[2] and Wei Li[3]

[1]School of Science, East China University of Technology, Nanchang, China
[2]Faculty of Civil and Architecture Engineering, East China University of Technology, Nanchang, China
[3]College of Civil Engineering and Architecture, Wenzhou University, Wenzhou, China

Correspondence should be addressed to Wei Li; liw1981@126.com

Received 2 December 2021; Revised 2 February 2022; Accepted 7 February 2022; Published 3 March 2022

Academic Editor: Shengwen Tang

The experimental studies on the axial compression behaviors of rubberized concrete-filled square steel tubular columns after exposed to high temperatures were investigated in this paper. Ten specimens, including nine rubberized concrete-filled square steel tubular columns with 5%, 10%, and 20% rubber aggregate replacement rate, respectively, and one natural concrete-filled square steel tubular column with 0% rubber aggregate replacement rate after exposed to 20°C, 200°C, 400°C, 600°C, and 800°C for 30 min, 90 min, and 180 min, respectively, were subjected to test. The failure mode and load-displacement curve of the specimens were displayed and analyzed. The test results showed that the higher the replacement rate was, the smaller the ultimate load the specimen could bear and the better the ductility exhibited. The stiffness change of the specimen was not obvious, and the stiffness of the specimen with 20% rubber aggregate replacement rate decreased significantly. With the increase of temperature, the ultimate load and stiffness of the specimen decreased, and the stiffness of the specimen decreased greatly at 800°C. Based on the experimental results, a formula for calculating the bearing capacity of rubberized concrete-filled square steel tubular column after exposed to high temperatures was proposed, and the calculated results were in good agreement with the experimental values.

1. Introduction

With the continuous development of China's industrial process, the contradiction between the shortage of natural resources and the rapid development of society is becoming increasingly fierce. Low-carbon green development will become the only way of social sustainable development. With the rapid development of the global automobile industry and transportation industry, the use of automobile tires has increased dramatically, and the output of waste tires is also increasing. According to the statistics of the World Health Organization, the world's waste tire inventory had reached 3 billion, with an amazing annual growth of one billion [1]. Waste rubber is not easy to degrade naturally, and direct landfill is easy to cause soil pollution. Incineration disposal will produce a large number of toxic and harmful gases, causing air pollution [2]. Such a huge amount of waste rubber cannot be effectively disposed, which is not only a great waste of resources but also contrary to the basic national policy of sustainable development. Therefore, it is necessary to make rational use of waste rubber resources to turn waste into treasure and promote the sustainable development of economy.

Although the concrete material commonly used in engineering has high strength, it also has brittleness, which leads to its strength not being fully utilized [3–6]. It was found that the new rubberized concrete had the advantages of lightweight, elastic shock absorption, noise reduction, sound insulation, heat insulation, strong deformation energy consumption, and good durability [7]. Gholampoura et al. [8] showed that the compressive strength of rubberized concrete decreased rapidly with the increase of rubber content. Ma [9] found that the strength of rubberized concrete decreased with the increase of substitution rate, and the substitution rate had the strongest effect on the compressive strength. Although the addition of rubber could greatly improve the antifracture and deformation capacity of concrete, its compressive capacity and tensile capacity were lost. In order to solve this problem, the rubberized concrete-filled steel tube was chosen. Concrete-filled steel tube (CFST) referred to the core concrete poured inside the steel tube, which could resist the external load together with the steel tube and maintained the cooperative work. The rubberized concrete-filled steel tube was similar to the concrete-filled steel tube, only replacing the core ordinary concrete with rubberized concrete. The composite of steel tube and rubberized concrete had attracted much attention in the application of building structure reinforcement and new composite structure. Abendeh et al. [10] found that rubberized concrete-filled steel tube was more ductile than ordinary concrete-filled steel tube. Bengar and Shahmansouri [11] found that the addition of rubber in concrete-filled steel tube could improve the plasticity of members, which was conducive to absorbing and dissipating seismic energy and met the requirements of seismic resistance. High temperature had an important influence on the performance of structure engineering. In order to make the new type of rubberized concrete-filled steel tube columns applied in practical engineering, it was very necessary to study structural behavior of rubberized concrete-filled steel tube columns after high temperature.

Therefore, in this paper, the failure mode of rubberized concrete-filled square steel tubular columns after high temperature was studied through the axial compression, and the influence of rubber aggregate replacement rate, temperature, and constant temperature time on stiffness and ductility was analyzed, and a calculation formula for the load bearing capacity of rubberized concrete-filled was presented and discussed.

2. Experimental Program

2.1. Materials and Mix Proportions. The rubberized concrete mixture was designed according to the Chinese code JGJ55-2011 (2011) [12], where common Portland cement (C) with a strength of 32.5 MPa as well as natural coarse aggregate (CA), fine aggregate (FA), and tap water (W) was used. The coarse aggregate had a size fraction of 5–20 mm. The fine aggregate had a fineness modulus of 2.7 and 0.6% moisture content. In the mixture, the fine aggregate, i.e., sand, was replaced with rubber aggregate (RA) by different percentages with 0%, 5%, 10%, and 20% in total mass of fine aggregate, respectively. The rubber aggregate had a size fraction of 0.825 mm and apparent density of 1020 kg/m^3. The mix proportions of rubberized concrete are presented in Table 1. In the names assigned to the mixtures, letter C shows the presence of rubber aggregate in the concrete mixture with the following number giving its percentage replacing the fine aggregate in mass. Square steel tubes (Q235) with a thickness of 3 mm, sectional width of 120 mm, and height of 300 mm were used. The mechanical properties of non-heated and heated steel tubes are listed in Table 2.

2.2. Specimen Preparation. For this experiment, ten steel tubular columns, including nine rubberized concrete-filled square steel tubular columns and one normal concrete-filled square steel tubular column, were designed and subjected to axial compression. The main variables in the test included the following:

(i) Rubber aggregate replacement rate (r): 0, 5%, 10%, and 20%.
(ii) Temperatures (T): 20°C, 200°C, 400°C, 600°C, and 800°C.
(iii) Time (t): 30 min, 90 min, and 180 min.

A summary of specimen details is presented in Table 3, where f_{cu} is the compressive cube strength of concrete and N_u is the tested ultimate strength of the columns. In the table, the number after R represents the rubber aggregate replacement rate, the number after T represents the heated temperature, and the number after t represents the time for maintaining target temperature.

2.3. Testing Methods. The specimens were heated in a high-capacity electrical furnace with a maximum heating temperature of 900°C. The heating rate was 10° C/min. After the required temperature of 200°C, 400°C, 600°C, and 800°C was reached, the temperature was maintained for 30 min, 90 min, or 180 min. Then, the specimens were cooled at ambient temperature before testing. The axial compression behavior of the columns was tested by a YAW-3000 microcomputer-controlled electro-hydraulic servo tester with 3000 kN compressive capacity. Four strain gauges glued at the mid-height position of the columns with an interval of 90° and two linear variable displacement transducers (LVDTs) were used to measure the longitudinal deformation. The test setup of the rubberized concrete-filled square steel tubular columns under axial compression is shown in Figure 1.

3. Results and Discussion

3.1. Visual Observations and Failure Modes. During the heating process, when the furnace temperature reached about 200°C, a small amount of water vapor continued to emerge from the exhaust hole of the furnace. When the temperature reached 400°C, the water vapor emission was the most obvious, accompanied by pungent odor. The higher the replacement rate was, the stronger the pungent odor was. When the temperature reached about 600°C, the steam did not come out after a period of time. The results showed that there was no distortion and bulging phenomenon for the columns after exposed to high temperatures, and the integrity of the columns remained relatively intact. With the increase of temperature, the surface color of the outer steel tubes clearly differed. At the temperature of 200°C, the color of the steel tube was slightly darker than that at 20°C (room temperature). When the temperature was higher than 400°C, it was visibly darker. The higher the temperature was, the darker the color was. When the temperature reached 800°C, the color of the steel tube was black.

Table 1: Mix proportion of rubberized concrete.

No.	Replacement (%)	RA (kg·m^{-3})	C (kg·m^{-3})	FA (kg·m^{-3})	CA (kg·m^{-3})	W (kg·m^{-3})
R0	0	0	418	613	1164	205
R5	5	30.7	418	582.3	1164	205
R10	10	61.3	418	551.7	1164	205
R20	20	122.6	418	490.4	1164	205

Table 2: Mechanical properties of square steel tube.

T (°C)	t (min)	fy (MPa)	fu (MPa)	E (GPa)
20	—	498	609	210
200	180	401	490	207
400	180	379	463	203
600	180	278	338	199
800	180	254	311	192
600	30	452	548	205
600	90	313	381	201

Note. T. = temperature, t = time, fy = yield strength, fu = ultimate strength, and E = Young's modulus.

Table 3: Details of specimens and experiment results.

Specimen	r (%)	T (°C)	t (min)	f_{cu} (MPa)	N_u (kN)
R10T20	0	20	—	38.2	741.3
R10T200t180	10	200	180	34.6	647.6
R10T400t180	10	400	180	27.8	518.3
R10T600t180	10	600	180	19.1	492.1
R10T800t180	10	800	180	8.1	424.7
R0T600t180	0	600	180	27.3	643.9
R5T600t180	5	600	180	21.9	549.4
R20T600t180	20	600	180	15.4	485.4
R10T600t30	10	600	30	34.9	577.2
R10T600t90	10	600	90	26.6	518.3

Figure 1: Test setup.

The failure mode of rubberized concrete-filled square steel tubular columns was not much different from that of ordinary concrete-filled steel tubular columns. It could be divided into elastic stage, elastic-plastic stage, and failure stage. The shear failure of non-parallel oblique circular bulge appeared at the top, middle, and bottom [13], as shown in Figure 2. The overall yield of the steel tube was serious, but no obvious crack appeared on the surface of top or bottom concrete. At the initial stage of loading, the specimen was in the elastic stage, there was no obvious change on the surface of the specimen, and only some intermittent extrusion and collision sound could be heard. With the increase of the loading, the specimen was in the elastic-plastic stage, the volume of the steel tube column was slightly expanded due to compression, and the specimen exhibited irregular steel wall buckling. When the specimen was in the failure stage, the convex part became thicker and thicker, showing a semi-circle shear failure. The typical failure mode of the specimens is shown in Figure 3.

3.2. Load-Displacement Curves. The load-displacement curve of the rubberized concrete-filled square steel tubular columns after exposed to different temperatures is shown in Figure 4(a). It can be seen from Figure 4(a) that with the increase of temperature, the ultimate load of the specimen decreased gradually, the overall performance of the specimen deteriorated, and the yield point moved down when it entered the yield stage.

The load-displacement curve of the rubberized concrete-filled square steel tubular columns with different rubber aggregate replacement rates after exposed to high temperature is shown in Figure 4(b). It can be seen that the higher

Figure 2: The shear failure of oblique circular bulge.

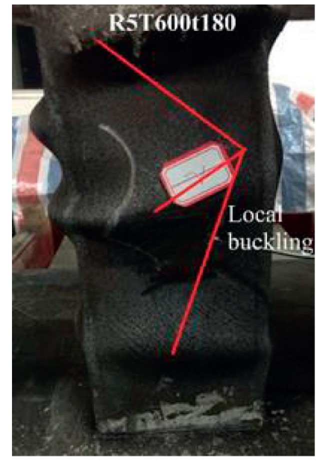

Figure 3: The typical failure mode of tested specimen.

the rubber aggregate replacement rate was, the smaller the ultimate load the specimen could bear and the faster it reached the peak load value during the loading process. This was because the strength for the concrete with higher rubber aggregate replacement rate was lower, and it made the ultimate strength of the specimens decreased [14].

The load-displacement curve of the rubberized concrete-filled square steel tubular columns after exposed to high temperature at different constant temperature time is shown in Figure 4(c). With the increase of constant temperature time, the ultimate load of the specimen decreased. The ultimate loads of specimens with constant temperature of 600°C for 30 min, 90 min, and 180 min are 577.2 kN, 518.3 kN, and 492.1 kN, respectively. That is, the constant temperature time had a great influence on the ultimate strength of rubberized concrete-filled square steel tubular columns.

3.3. Axial Stiffness. The axial stiffness of the rubberized concrete-filled square steel tubular columns can be defined as follows [15]:

$$E_{sc}A_{sc} = \frac{\sigma}{\varepsilon}A_{sc}, \qquad \sigma = \frac{N}{A_{sc}}. \tag{1}$$

According to the definition, the slope of load-displacement curve can reflect the change of axial stiffness. It can be seen from Figure 4(a) that the axial stiffness of the tested specimens decreased with increasing temperature from 20°C to 800°C. With the load increasing until the steel tube yield, the load-displacement curves of the specimens with different temperatures reached the peak value and then began to decrease, the axial stiffness decreased, and finally the change of the stiffness tended to be stable. In addition, the stiffness of specimens at 600°C and 800°C decreased significantly, which indicated that the high-temperature environment of 600°C and 800°C would greatly reduce the stiffness of rubberized concrete-filled square steel tubular columns.

As shown in Figure 4(b), the load-displacement curves of three types of specimens with 0%, 5%, and 10% replacement rate in the elastic stage were linear, which indicated that the axial stiffness of the specimens was basically the same, while the axial stiffness of the specimens with 20% substitution rate was significantly reduced. It could be concluded that the rubber aggregate replacement rate less than 10% had little effect on the stiffness of rubberized concrete-filled square steel tubular columns after high temperature, but the rubber aggregate replacement rate with 20% greatly reduced the stiffness of specimens. In order to ensure the stiffness of this composite column in practical engineering application, it was suggested that the rubber aggregate replacement rate should be controlled within 10%.

As shown in Figure 4(c), the load-displacement curve of the three specimens had similar overall trend, and the curve in elastic stage was basically the same without obvious increase or decrease, indicating that the stiffness of the specimens was basically consistent. It can be seen that constant temperature time had little influence on the stiffness of the rubberized concrete-filled square steel tubular columns.

3.4. Calculation Formula of the Ultimate Bearing Capacity. The effects of rubber aggregate replacement rate, temperature, and heating time on axial compression behavior of rubberized concrete-filled square steel tubular columns were studied. The influence coefficients of rubber aggregate replacement rate and temperature determined by experimental parameters were introduced to calculate the ultimate bearing capacity. Based on the experimental data, the ultimate bearing capacity of rubberized concrete-filled square steel tubular columns after exposed to high temperature was calculated as follows [16–20]:

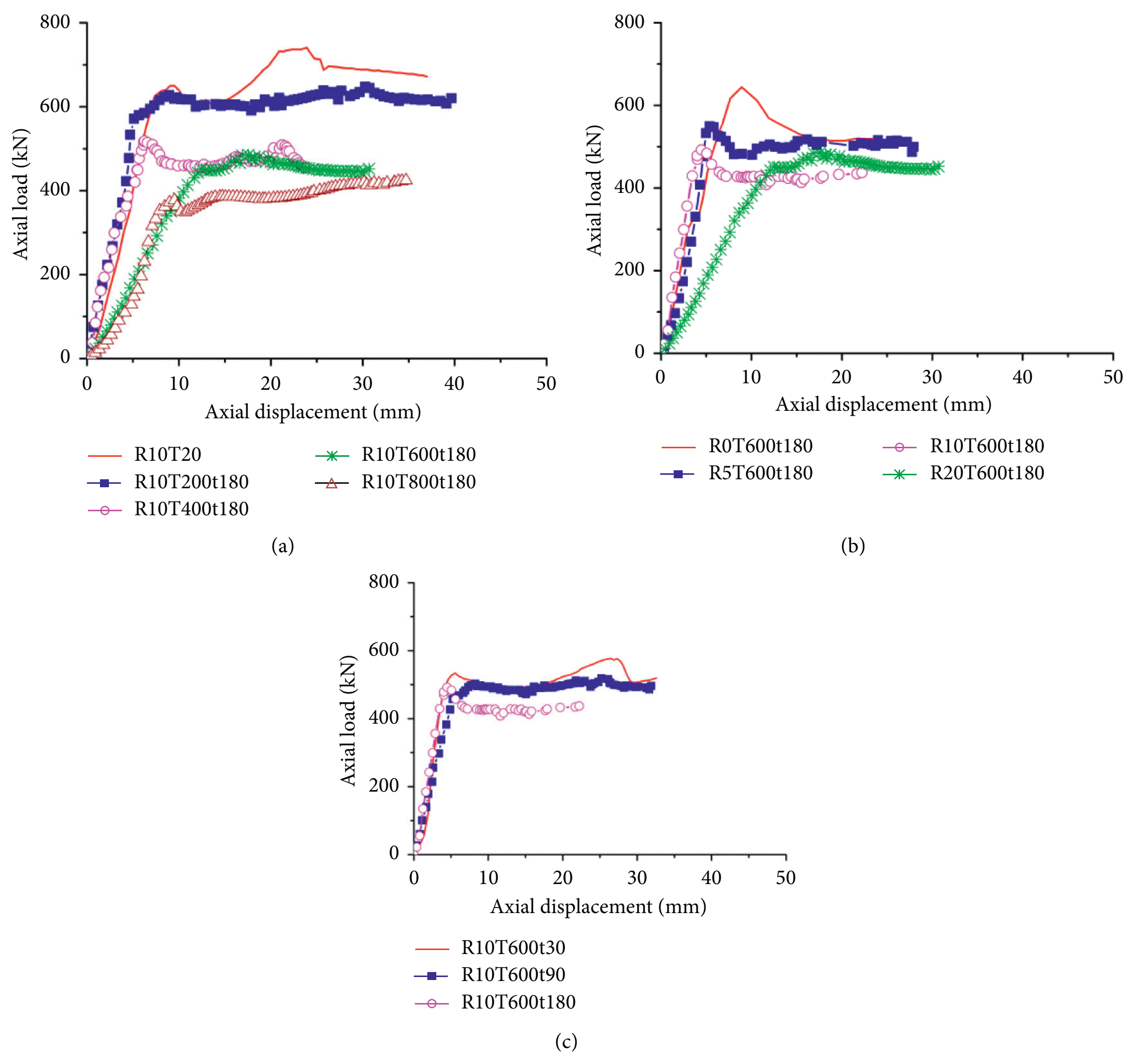

Figure 4: Load-displacement curves of the tested specimens.

$$B = \frac{0.131 f_y}{213} + 0.723,$$

$$C = \frac{-0.070 f_{ck}}{14.4} + 0.026,$$

$$K_r = 0.98 + 0.03r - 0.007r^2 + 2.54 \times 10^{-4} r^3 \; (0 \le r \le 20),$$

$$K_T = 1.06 - 6.17 \times 10^{-4} T \left(20^\circ\mathrm{C} \le T \le 800^\circ\mathrm{C}\right),$$

$$K_t = 1 - 0.181 \frac{t - 180}{180} \; (30 \le t \le 180),$$

$$\xi = \frac{A_s \times f_y}{A_c \times f_{ck}},$$

$$f_{sc} = K_r K_T K_t \left(1.212 + B\xi + C\xi^2\right) f_{ck},$$

$$N_u = A_{sc} f_{sc}, \qquad (2)$$

where B is the yield stress of steel tube coefficient, f_y is the yield stress of steel tube, C is the compressive strength of concrete coefficient, f_{ck} is the compressive strength of concrete, K_r is the rubber aggregate replacement rate coefficient, r is the rubber aggregate replacement rate, K_T is the heated temperature coefficient, T is the heated temperature, K_t is the heating time coefficient, t is the heating time, ξ is the confinement factor defined as the ratio of the plastic capacity of the empty steel tube to that of the unconfined concrete core, A_s is the cross-sectional area of steel tube, A_c is the cross-sectional area of concrete, f_{sc} is the compressive strength of square rubberized concrete-filled square steel tubular columns, A_{sc} is the cross-sectional area of square rubberized concrete-filled square steel tubular columns, and N_u is the ultimate strength of square rubberized concrete-filled square steel tubular columns.

The calculation values of the ultimate bearing capacity were compared with the experiment values, and the comparison results are shown in Table 4, where N_{cal} represents calculation value. The mean value of $N_{\mathrm{cal}}/N_{\mathrm{u}}$ was 1.01, max value was 1.13, and min value was 0.91. Also, it can be seen

Table 4: Comparison results of the tested specimens.

Specimen	N_{cal} (kN)	N_u (kN)	N_{cal}/N_u
R10T20	752.5	741.3	1.02
R10T200t180	672.7	647.6	1.04
R10T400t180	584.1	518.3	1.13
R10T600t180	495.4	492.1	1.00
R10T800t180	406.8	424.7	0.96
R0T600t180	582.2	643.9	0.91
R5T600t180	586.2	549.4	1.06
R20T600t180	482.4	485.4	0.99
R10T600t30	570.2	577.2	0.99
R10T600t90	540.3	518.3	1.04

that the accuracy with which the equation predicted the ultimate bearing capacity of rubberized concrete-filled square steel tubular columns after exposed to high temperatures was reasonable.

4. Conclusions

In this experiment, the axial compression behavior of rubberized concrete-filled square steel tubular columns after exposed to high temperature was studied. According to the experimental results, the following conclusions were drawn:

(1) The higher the replacement rate was, the smaller the ultimate load of rubberized concrete-filled square steel tubular columns after high temperature was. When the replacement rate was less than 10%, with the increase of the replacement rate, the stiffness of the specimen did not change significantly, but the ductility coefficient increased, and the ductility became better. When the replacement rate reached 20%, the stiffness and ductility of the specimen decreased obviously, so it was suggested that the replacement rate should be controlled within 10% in practical engineering application.

(2) With the increase of constant temperature, the ultimate load of rubberized concrete-filled square steel tubular columns decreased and the yield point moved down. When the constant temperature increased from 20°C to 600°C, the axial stiffness of the specimen remained the same basically, and the ductility coefficient increased gradually. The specimen had better ductility at high temperature. However, the stiffness of the specimen would be greatly reduced at 800°C.

(3) After analyzing the ultimate bearing capacity of each specimen under different influence parameters, by introducing the influence coefficient of replacement rate and constant temperature, the calculation formula of ultimate bearing capacity of rubberized concrete-filled square steel tubular columns was proposed. The calculated results were in good agreement with the experimental ones.

Data Availability

The data used to support the findings of this study are included within the article.

Conflicts of Interest

The authors declare that they have no conflicts of interest regarding the publication of this paper.

Acknowledgments

This study was supported by the Chinese National Natural Science Foundation (nos. 52068001 and 51608435), the Project of Academic and Technological Leaders of Major Disciplines in Jiangxi Province (no. 20204BCJL2037), the Natural Science Foundation of Jiangxi Province (no. 20202ACBL214017), and the Key R&D Program of Jiangxi Province (no. 20212BBG73002). The authors are grateful for the support.

References

[1] K. Bisht and P. V. Ramana, "Evaluation of mechanical and durability properties of crumb rubber concrete," *Construction and Building Materials*, vol. 155, pp. 811–817, 2017.

[2] E. Guneyisi, M. Gesoglu, K. Mermerdas, and S. Ipek, "Experimental investigation on durability performance of rubberized concrete," *Advances in concrete construction*, vol. 2, no. 3, pp. 193–207, 2014.

[3] W. Lei, X. Zeng, H. Yang, and X Lv, "Investigation and application of fractal theory in cement-based materials: a review," *Fractal and Fractinal*, vol. 5, no. 4, p. 247, 2021.

[4] L. Wang, X. Lu, L. Liu et al., "Influence of MgO on the hydration and shrinkage behavior of low heat Portland cement-based materials via pore structural and fractal analysis," *Fractal and Fractional*, vol. 6, no. 1, p. 40, 2022.

[5] F. X. Guo, H. M. Yang, Y. Wang, and W. Lei, "Comparison of fly ash, PVA fiber, MgO and shrinkage-reducing admixture on the frost resistance of face slab concrete via pore structural and fractal analysis," *Fractals*, vol. 29, no. 2, Article ID 2140002, 2021.

[6] J. Huang, W. Li, D. Huang et al., "Fractal analysis on pore structure and hydration of magnesium oxysulfate cements by first principle, thermodynamic and microstructure-based methods," *Fractal and Fractional*, vol. 5, no. 4, p. 164, 2021.

[7] A. S. M Mendis, S Al-Deen, and M Ashraf, "Effect of rubber particles on the flexural behaviour of reinforced crumbed rubber concrete beams," *Constr.Build. Mater.*vol. 154, pp. 644–657, 2017.

[8] A. Gholampoura, A. H. Gandomib, and T. Corrigendum, "New formulations for mechanical properties of recycled aggregate concrete using gene expression programming".

Construction and Building Materials," vol. 278, Article ID 122930, 2021.

[9] N. Ma, "Experimental study on mechanical properties of rubber concrete," *Subgrade Engineering*, vol. 3, pp. 79–82, 2016.

[10] R. Abendeh, H. S. Ahmad, and Y. M. Hunaiti, "Experimental studies on the behavior of concrete-filled steel tubes incorporating crumb rubber," *Journal of Constructional Steel Research*, vol. 122, pp. 251–260, 2016.

[11] H. A Bengar, A. A. Shahmansouri, Post-fire behavior of unconfined and steel tube confined rubberized concrete under axial compression," *Structures*, vol. 32, pp. 731–745, 2021.

[12] JGJ55–2011, *Specification for Mix Proportion Design of Ordinary concrete*, China Building Industry Press, Beijing, China, 2011.

[13] C. Jie, Z. Sumei, W. Yuyin, and Y Geng, "Axial compressive behavior of recycled concrete filled steel tubular stubcolumns with the inclusion of crushed brick," *Structures*, vol. 26, pp. 271–283, 2020.

[14] M. Nematzadeh, "Amirhossein Karimi, Saber Fallah-Valukolaee. Compressive performance of steel fiber-reinforced rubberized concrete core detached from heated CFST. Construction and Building Materials," vol. 239, Article ID 117832, 2020.

[15] M. Cai, "Xiaojun Ke, Deyi Xu. Study on axial compressive stiffness of RAC-encased RACFST composite columns," *Thin-Walled Structures*, vol. 162, Article ID 107570, 2021.

[16] L Han and Y Yang, *Modern Concrete Filled Steel Tubular Structure Technology*, pp. 1-2, China Construction Industry Press, Beijing, 2007.

[17] S Zhong, "Concrete filled steel tubular structure," pp. 1–5, Tsinghua University Press, Beijing, 2003.

[18] EC4, "Design of Composite Steel and Concrete Structures-Part 1.1: General Rules and Rules for Buildings, European Committee for Standardization," Brussels, Belgium, 2004.

[19] AIJ, "Recommendations for design and construction of concrete filled steel tubular structures. Architectural Institute of Japan (AIJ)," Tokyo, Japan, 2008.

[20] ANSI/AISC360-10, "Specification for Structural Steel Buildings," *American Institute of Steel Construction*, Chicago, IL, USA, 2010.